

Optimization of sulfuric acid hydrolysis conditions for preparation of nanocrystalline cellulose from enzymatically pretreated fibers

Facundo Beltramino · M. Blanca Roncero ·
Antonio L. Torres · Teresa Vidal · Cristina Valls

Received: 18 September 2015 / Accepted: 29 February 2016 / Published online: 22 March 2016
© Springer Science+Business Media Dordrecht 2016

Abstract Preparation of nanocrystalline cellulose (NCC) by 62 and 65 % wt. sulfuric acid hydrolysis of cellulase-pretreated fibers was optimized to obtain the highest yield by applying two statistical plans. At optimal conditions (10 U/g odp cellulase, 25 min hydrolysis, 47 °C, 62 wt.% H₂SO₄), high yields (≥ 80 %) were obtained, including an increase of ~ 9 points due to the enzyme. Optimal conditions produced nanosized particles of around ~ 200 nm with reduced surface charge and sulfur content. The optimization allowed reduction of hydrolysis time by 44 % and increase of yield by more than 10 points compared with results in previous work. The effects of cellulase pretreatment were noticeable even under aggressive hydrolysis conditions, emphasizing its possibilities. Zeta potential and polydispersity index indicated that all studied conditions led to good-quality final products, with values around -50 mV and 0.2, respectively. Transmission electron

microscopy (TEM) analysis confirmed the presence of NCC. Fourier-transform infrared (FTIR) spectroscopic analysis provided evidence that cellulase treatment increased the crystallinity of both cellulose fibers and NCC, as well as fiber accessibility, supporting the other analyses of NCC.

Keywords Nanocrystalline cellulose · Cellulose nanocrystals · Optimization · Cellulase · Enzymatic treatment · Yield increase

Abbreviations

C	Cellulase-treated fibers
C_NCC	NCC obtained from cellulase-pretreated fibers
CMC	Carboxymethylcellulose
FTIR	Fourier-transform infrared
KC	Control fibers
KC_NCC	NCC obtained from control fibers
NCC	Nanocrystalline cellulose
Opd	Oven-dried pulp
LOI	Lateral order index
TCI	Total crystallinity index
U	Enzymatic activity unit

Introduction

Over recent decades, human activities and increasing energy demands have led to overuse of nonrenewable

F. Beltramino · M. B. Roncero (✉) ·
A. L. Torres · T. Vidal · C. Valls
CELBIOTECH_Paper Engineering Research Group,
Universitat Politècnica de Catalunya (UPC,
BarcelonaTech), Colom 11, E-08222 Terrassa, Spain
e-mail: facundo.beltramino@etp.upc.edu

M. B. Roncero
e-mail: roncero@etp.upc.edu

A. L. Torres
e-mail: torres@etp.upc.edu

resources such as coal, petroleum, and natural gas, dramatically increasing the pollution generated by these activities (Neto et al. 2013). This scenario of growing environmental concerns has resulted in a shift in society towards use of natural renewable resources to fulfill our needs (Neto et al. 2013). Cellulose, being one of the most important natural polymers on Earth and virtually inexhaustible, is a key source of sustainable materials suitable for industrial applications (Klemm et al. 2011).

Physically, cellulose is a fibrous, tough, water-insoluble substance that plays an essential role in maintaining the structure of plant cell walls (Habibi et al. 2010). Chemically, cellulose consists of a linear homopolymer of β -D-glucopyranose units linked by glycosidic bonds, with a repeating subunit consisting of two linked glucose units corkscrewed 180° with respect to each other (Habibi et al. 2010). Cellulose chains aggregate into larger structures, i.e., microfibrils. These microfibrils present crystalline ordering, disrupted by amorphous regions. Degradation of these defects leads to release of needle-like particles consisting of crystalline regions, denominated nanocrystalline cellulose (NCC) or cellulose nanocrystals (CNC) (Habibi et al. 2010). The interest in NCC lies in its outstanding mechanical properties at the nanoscale, making it a very interesting sustainable reinforcing agent for a variety of materials (Klemm et al. 2011). The chemical properties of NCC, which strongly depend on the preparation method used, determine its physicochemical behavior when incorporated into polymeric matrixes or other composites (Klemm et al. 2011). Applications for NCC include improvement of mechanical properties, modification of thermal properties, modification of barrier properties of nanocomposites, control of optical properties, and potential uses in biomedicine (Brinchi et al. 2013).

In literature, isolation of NCC has been carried out by diverse methods, traditionally characterized by low yields that reduce their economic and environmental efficiency. Studies such as those reported by Fan and Li (2012) and Chen et al. (2015) have addressed this topic, studying ways to increase the yield of sulfuric acid hydrolysis, the most widely used preparation method. Other methods, such as NCC preparation through enzymatic hydrolysis of cellulose in combination with chemical and/or mechanical treatments, have also been proposed by various authors (Filson et al. 2009; Anderson et al. 2014; Teixeira et al. 2015). These

methods usually lead to very low yields as well as uncharged particles that produce unstable suspensions, reducing their industrial potential. Previous studies by our group (Beltramino et al. 2015a) demonstrated that the combination of enzymatic pretreatment plus sulfuric acid hydrolysis could increase the yield of NCC isolation while influencing other properties and leading to suspensions of electrically charged nanoparticles with good stability. Hence, introduction of biotechnology would improve the efficiency of such isolation and also permit a reduction of the environmental impact of sulfuric acid hydrolysis. In previous work, we observed that the magnitude of the effects of enzymatic pretreatment of NCC is largely dependent on the hydrolysis conditions used for isolation. Experimental designs have been used in literature to optimize process conditions (Valls and Roncero 2009; Valls et al. 2010). In this work, two experimental plans were carried out with two different acid doses to study the influence of three variables, namely the presence of enzymatic pretreatment, hydrolysis time, and hydrolysis temperature, on NCC preparation. To the best of our knowledge, this is the first optimization of this kind performed on enzymatically pretreated fibers. The aim of this work is both to maximize the NCC yield from enzymatically pretreated fibers and to assess the relation between the effects of enzymatic pretreatment and the intensity of acid hydrolysis.

Materials and methods

Fibers, enzyme, and enzymatic treatment

Cotton linters, provided by Celsur (Spain), were used as cellulose source (cellulose content $97.7 \pm 0.3\%$), and named “initial fibers.” Cellulase provided by Fungal Bioproducts (Spain) was used for treatments. The activity, as U per gram of enzyme stock, i.e., the amount of enzyme degrading $1 \mu\text{mol}$ carboxymethylcellulose (CMC) per minute, was 1700 U/g CMC case units. Enzymatic treatment (C) was performed with a 10 U/g oven-dried pulp (odp) dose for 24 h in a 4-L cylindrical reactor with agitation produced by blades rotating at 30 rpm. Treatment was performed at 55°C , 5 % consistency, and pH 5 as maintained using 50 mM acetate buffer. Control fibers, named “KC” (0 U/g odp), were obtained using the same conditions as for enzymatic treatment, but without enzyme addition.

Experimental designs

The relations between process variables in NCC preparation via sulfuric acid hydrolysis and the effects of C were studied via two experimental designs using two different acid concentrations. For this purpose, three independent variables were studied: X1 (cellulase) with values of 0 U/g odp, i.e., absence, and 10 U/g odp, i.e., presence; X2 (acid hydrolysis time) with values of 25 and 50 min; X3 (acid hydrolysis temperature) with values of 47 and 60 °C. For cellulase dose of 0 U/g odp, we used KC (control fibers) as cellulose source. These independent variables were coded as -1 or $+1$, both for direct comparison of coefficients and to better understand the effect of each variable on the responses (Table 1). Therefore, two 2^3 complete factorial experimental designs were used, requiring eight experiments each. The aim was to determine only the individual effects of each of the three variables and their interactions, as described in literature (Valls et al. 2010). Runs in factorial designs were randomized to reduce the impact of bias on the results. Data was then analyzed using a Microsoft Excel spreadsheet to implement the stepwise

backward regression method and discard all terms with probability (p value) lower than 0.05 (Table 2).

NCC preparation

Nanocrystalline cellulose was obtained by controlled hydrolysis by sulfuric acid, using a protocol proposed by Dong et al. (1998). Before acid hydrolysis, fibers were fluffed and oven-dried. Typically, 1.5 g fibers weighed immediately from desiccator was hydrolyzed using 62 or 65 wt.% sulfuric acid received as 96 % PA-ISO (Panreac, Spain) and diluted before use. An acid-to-fibers ratio of 10:1 (10 mL/1 g cellulose) was used, and the reaction was conducted with magnetic stirring. Other reaction conditions differed for each sample as indicated in Table 1. The hydrolysis reaction was quenched using chilled (4 °C) distilled water to dilute samples tenfold while cooling them on an ice bath. After this, suspensions were centrifuged at 6000 rpm for 15 min, and supernatant was discarded only if not turbid to avoid sample loss. The centrifugation step was repeated until the supernatant became turbid and could not be discarded. After centrifugation, a sonication step was carried out for NCC

Table 1 Experiments of both statistical plans with their conditions and obtained experimental values

	X1	X2	X3	Cellulase (U/g odp)	Time (min)	Temperature (°C)	Yield (%)	Z average (nm)	Surface charge (meq/g)
Sulfuric acid 65 wt.%									
Y1	-1	-1	-1	0	25	47	73.5 ± 0.2	184.8 ± 5.6	0.164 ± 0.02
Y2	1	-1	-1	10	25	47	84.1 ± 0.5	214.7 ± 34.3	0.188 ± 0.009
Y3	-1	1	-1	0	50	47	54.5 ± 0.3	97.5 ± 1	0.190 ± 0.002
Y4	1	1	-1	10	50	47	62.2 ± 0.2	98.9 ± 2.8	0.222 ± 0.001
Y5	-1	-1	1	0	25	60	63.3 ± 0.2	76.7 ± 1.2	0.265 ± 0.014
Y6	1	-1	1	10	25	60	64.9 ± 0.2	79.7 ± 2.3	0.225 ± 0.013
Y7	-1	1	1	0	50	60	64.8 ± 0.5	69.3 ± 2.3	0.269 ± 0.008
Y8	1	1	1	10	50	60	65.8 ± 0.5	80.2 ± 2	0.271 ± 0.016
Sulfuric acid 65 wt.%									
Y1	-1	-1	-1	0	25	47	24.4 ± 0.1	89.2 ± 1.6	0.227 ± 0.005
Y2	1	-1	-1	10	25	47	25.8 ± 0.6	92.3 ± 3.6	0.216 ± 0.009
Y3	-1	1	-1	0	50	47	27.4 ± 0.4	81.6 ± 5.7	0.245 ± 0.01
Y4	1	1	-1	10	50	47	27.7 ± 0.3	93.4 ± 1.9	0.188 ± 0.011
Y5	-1	-1	1	0	25	60	27.8 ± 0.2	72.6 ± 0.6	0.222 ± 0.01
Y6	1	-1	1	10	25	60	30.3 ± 0.3	81.5 ± 1.4	0.232 ± 0.011
Y7	-1	1	1	0	50	60	26.8 ± 0.2	66.6 ± 1.6	0.241 ± 0.004
Y8	1	1	1	10	50	60	26.3 ± 0.4	81.6 ± 1.5	0.216 ± 0.014

Table 2 *p* values for each variable for the different models obtained using each acid dose

	Yield		Z average		Surface charge	
	62 wt. %	65 wt. %	62 wt. %	65 wt. %	62 wt. %	65 wt. %
X1	0.0196	0.0055	–	0.0024	–	0.0047
X2	0.0059	–	0.0014	0.0231	0.0269	–
X3	0.0352	0.0022	0.0005	0.0012	0.0012	0.0490
X1X2	–	0.0047	–	0.0164	–	0.0054
X1X3	0.0339	–	–	0.0433	0.0440	0.0161
X2X3	0.0047	0.0008	0.0018	–	–	–
X1X2X3	–	0.0219	–	–	–	–

dispersion, using a UP100H ultrasonic processor (Hielscher, Germany) at 100 % amplitude and 0.75 cycles for 25–30 min on an ice bath to prevent heating, which is known to be able to cause desulfation (Dong et al. 1998). Resuspended samples were then dialyzed against distilled water using a 10-kDa Thermo Fischer dialysis membrane for 3 days. After dialysis, the sonication step was repeated for 20 min. Finally, samples were filtered through a Whatman® 41 membrane. NCC obtained from cellulase-pretreated and control fibers is denoted as C_NCC and KC_NCC, respectively.

Characterization of samples

Cellulose fiber length of initial, control (KC), and cellulase-treated (C) fibers was measured in accordance with Technological Association of the Pulp and Paper Industry (TAPPI) Standard T271 using a Kajaani FS300 fiber analyzer (Metso Automation, Finland).

Yield of hydrolysis was determined by drying 25 mL NCC suspension at 60 °C in an air circulating oven and determining the NCC mass after water evaporation, a procedure similar to those used by Fan and Li (2012) and Martínez-Sanz et al. (2015). Solids content in suspension was calculated and yield expressed as % initial fiber mass. Values are given as the average of three independent determinations for each sample.

The particle size distribution of samples was determined by dynamic light scattering (DLS) at room temperature (25 °C) using a particle size analyzer (DL135, Cordouan Technologies, France). NCC suspensions (0.1–0.5 % w/v) were placed directly in the measuring cell. The laser power was adjusted for each sample to obtain a count of around 2000 particles/s.

Data were obtained in cummulants mode with three independent measurements carried out for each sample.

NCC surface charge was determined using a PCD03PH particle charge detector (Mütek, Germany). Suspensions were titrated using a cationic polyelectrolyte [0001 N polydiallyldimethylammonium chloride (polyDADMAC), used as received from Mütek]. Surface charge density was calculated according to the following formula:

$$\text{Surface charge} \left(\frac{\text{meq}}{\text{g}} \right) = \frac{V \times C}{\text{wt}},$$

where *V* and *C* are the volume and concentration of titration agent (polyDADMAC), respectively, and *wt* is the weight of NCC sample.

NCC sulfur content was determined according to the procedure described in Abitbol et al. (2013). Briefly, a small sample of suspension was titrated using 1.25 mM NaOH standard solution (Panreac, Spain), recording conductivity values. The equivalence point corresponds to the amount of NaOH necessary to neutralize all sulfate groups attached to the NCC surface. Results were calculated as the mass % of atomic sulfur over NCC mass. Values are given as the average of three independent measurements for each sample.

Electrophoretic mobility of aqueous NCC suspensions (zeta potential) was determined using a Zeta-master model ZEM (Malvern Instruments, UK). Data were averaged over 12 measurements. All samples were analyzed at room temperature.

Transmission electron microscopy (TEM) was used to examine the NCC morphology using a protocol similar to that described elsewhere (Chen et al. 2015). Carbon-coated Cu grids were firstly glow-discharged for 30 s, then floated on 5-μL drops of NCC

suspensions (0.1–0.5 % w/v) for 5 min. After that, NCC was negatively stained by floating grids consecutively into two 50- μL drops of 2 % aqueous uranyl acetate for 30 s. Excess stain was removed by capillary action and gentle blotting. Samples were analyzed using a JEOL JEM-1010 transmission electron microscope operating at 80 kV.

Fourier-transform infrared (FTIR) spectra of samples were recorded at room temperature using a Spectrum 100 attenuated total reflection (ATR) FTIR spectrophotometer (PerkinElmer, USA). FTIR spectral analysis was conducted in the wavenumber range of 600–4000 cm^{-1} . A total of 64 scans were run at resolution of 1 cm^{-1} to collect each spectrum. Lateral order index (LOI) and total crystallinity index (TCI), proposed by O'Connor (1958) and Nelson and O'Connor (1964), were estimated from the ratio between the absorption peaks at 1430 and 890 cm^{-1} bands, and 1370 and 2900 cm^{-1} , respectively.

Results and discussion

Initial fibers and enzymatic treatment

Previous studies with the cellulase used in the present study showed that it was capable of substantially reducing fiber length and cellulose viscosity (Quintana et al. 2015a, b; Beltramo et al. 2015b). Figure 1 shows the length distribution of cellulase-pretreated cotton linters compared with initial and control fibers, with the amount of longer fibers (i.e., between 3.2 and 7.6 mm) reduced by 40 % and an increased amount of shorter ones. Also, greater homogeneity of fiber length was observed, as more fibers with intermediate lengths (groups between 0.5 and 2 mm) were counted, highlighting increased raw material quality. Control treatment (KC), on the other hand, did not seem to affect fiber length (Fig. 1). These macroscopic fiber modifications together with other chemical modifications of, e.g., viscosity or crystallinity (Beltramo et al. 2015a) produced by the enzyme are assumed to modify the acid–fiber interaction during acid hydrolysis.

Models for yield, average particle size, and surface charge

The experimental results obtained for NCC yield, average particle size, and surface charge are presented

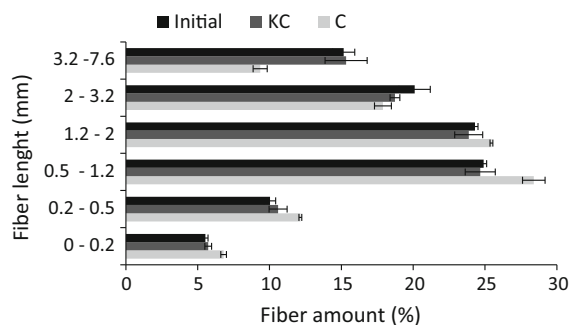


Fig. 1 Fiber length (mm) distribution of initial, cellulase-treated (C), and control (KC) fibers, indicated as % of total

in Table 1. Statistical models were built by fitting experimental data, and representative variables showed the p values presented in Table 2. The yield of the NCC preparation process is a key aspect for analysis, due to its implication for the overall cost of the process, with low yields implying greater consumption of biomass and reactants (Klemm et al. 2011; Wang et al. 2012). In this regard, the optimal yield of the process corresponds to the highest possible value. Models relating the yield for both 62 and 65 wt.% H_2SO_4 to other process variables were fit using Eqs. 1 and 2, respectively. Equation 1 shows that the yield was positively influenced by cellulase presence (X1), negatively by reaction time (X2) and temperature (X3), positively by the two-way interaction between time and temperature, and negatively by the two-way interaction between cellulase and temperature. Equation 2 indicates that, for stronger acid dose, the reaction time did not independently influence the yield, but it interacted with cellulase presence and temperature, conditioning their influence.

$$\begin{aligned} \text{Yield (\%)} = & 66.65 + 2.61X1 - 4.82X2 - 1.93X3 \\ & + 5.4X2X3 - 1.96X1X3 \end{aligned} \quad (1)$$

$$(R^2 = 0.996)$$

$$\begin{aligned} \text{Yield (\%)} = & 27.06 + 0.47X1 + 0.74X3 \\ & - 0.51X1X2 - 1.24X2X3 \\ & - 0.23X1X2X3 \end{aligned} \quad (2)$$

$$(R^2 = 0.999)$$

Based on the obtained model, yield between 60 and 84 % was obtained with 62 wt.% sulfuric acid (Fig. 2a), and the presence of cellulase increased the process outcome by up to ~ 9 % compared with control fibers (KC), supporting evidence presented by

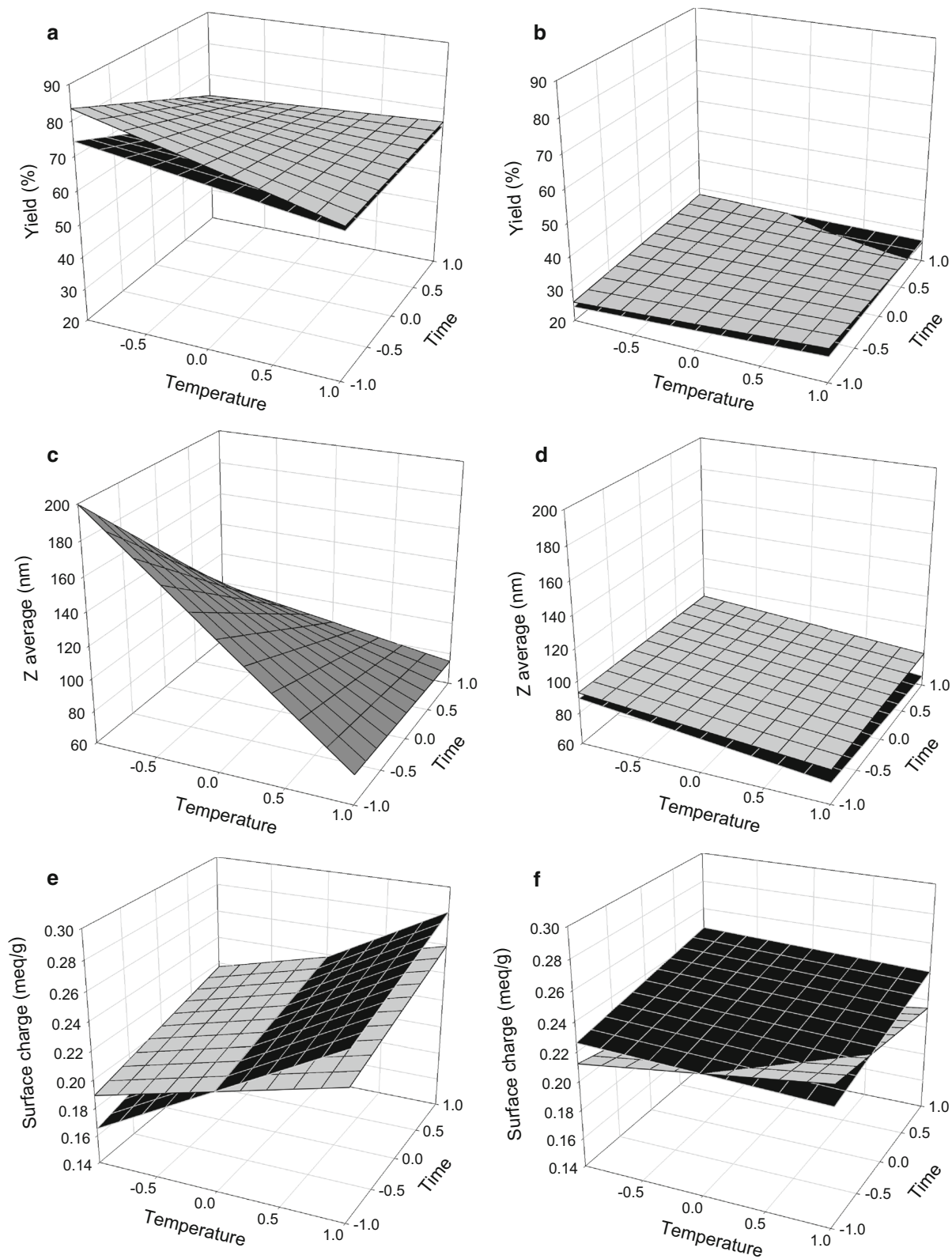


Fig. 2 Data predicted by models: yield (a), average size (c), and surface charge (e) with 62 wt.% sulfuric acid, and yield (b), average size (d), and surface charge (f) with 65 wt.% sulfuric acid. Grey and black charts represent data in presence and absence of cellulase, respectively

authors in a previous study (Beltramino et al. 2015a). This increase produced by cellulase was speculated to be caused by its preferential attack on amorphous cellulose regions of fibers, increasing their crystallinity and also facilitating the interaction with acid, reducing undesired cellulose mass loss (Beltramino et al. 2015a). Increases in time and temperature reduced the hydrolysis yield by up to 20 % in presence of cellulase, with a smaller effect in its absence. Yields with 65 wt.% acid were lower compared with 62 wt.% H₂SO₄, with values in the range of 24–30 %, due to the stronger depolymerization of cellulose produced by the higher acid concentration (Chen et al. 2015). Even in these conditions, cellulase was able to increase the yield by up to ~2.4 %, strongly highlighting the benefits of this pretreatment. At this stronger acid dose (65 wt.%), time and temperature had little influence on the yield.

Generally, DLS measurements do not provide a real measurement of average particle size, particularly when considering rod-like structures such as nanocrystalline cellulose (Fraschini et al. 2014). Nevertheless, these measurements provide a useful approximation to average particle size to establish comparisons between similar samples (Fraschini et al. 2014). The size of nanocrystalline cellulose is a key aspect to analyze to ensure the quality and characteristics of the obtained final product (Fraschini et al. 2014), as the NCC morphology can affect its performance when used in a particular application. These effects include, for instance, variations in permeability of membranes formed by NCC (Thielemans et al. 2009) or toxicity, as it has been found that smaller NCC particles show greater toxicity than larger ones (Yanamala and Farcas 2014). Also, we previously reported that the size and yield of NCC seem to be related (Beltramino et al. 2015a). Equations 3 and 4 indicate the models fitting the average Z values for 62 and 65 wt.% H₂SO₄, respectively. For 62 wt.% acid, we observed that the particle size was only affected (negatively) by reaction time and temperature and positively by their two-way interaction. Similar

influences were found for 65 wt.% acid, although in this case cellulase positively influenced this parameter, as did its interactions with both time and temperature.

With 62 wt.% sulfuric acid (Fig. 2c), we found that particle size was statistically not influenced by cellulase presence. Reaction time and temperature both reduced the average particle size by up to 60 %, due to enhanced cellulose degradation. With 65 wt.% acid (Fig. 2d), the average particle size was strongly reduced as a consequence of greater cellulose depolymerization produced by the acid, as observed by other authors (Fan and Li 2012). With this higher acid dose, cellulase presence increased the particle size up to 15 nm, while reaction time and temperature reduced the size, particularly in absence of enzymatic pretreatment.

$$Z \text{ average (nm)} = 112.7 - 26.2X_2 - 36.2X_3 + 24.5X_2X_3 \quad (3)$$

$$(R^2 = 0.976)$$

$$Z \text{ average (nm)} = 82.4 + 4.8X_1 - 1.6X_2 - 6.8X_3 + 1.9X_1X_2 + 1.1X_1X_3 \quad (4)$$

$$(R^2 = 0.998)$$

The surface charge of NCC is mainly due to sulfate groups esterified onto free superficial OH⁻ groups of cellulose during hydrolysis by sulfuric acid (Habibi et al. 2010; Abitbol et al. 2013). Because of this, NCC obtained using different acids, e.g., hydrochloric or hydrobromic, is mainly uncharged (Habibi et al. 2010). Thus, the NCC surface charge and sulfur content are expected to be related. Equations 5 and 6 fit the surface charge data for 62 and 65 wt.% acid, respectively. In

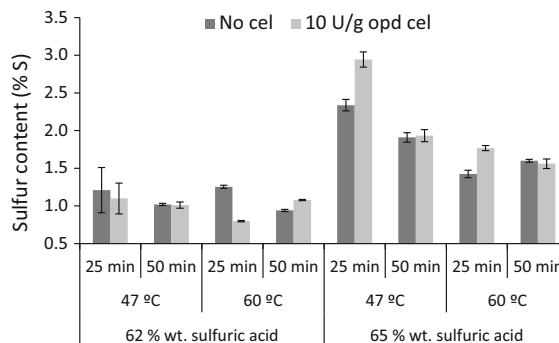


Fig. 3 Sulfur content (as % S) of samples at studied conditions in presence and absence of cellulase

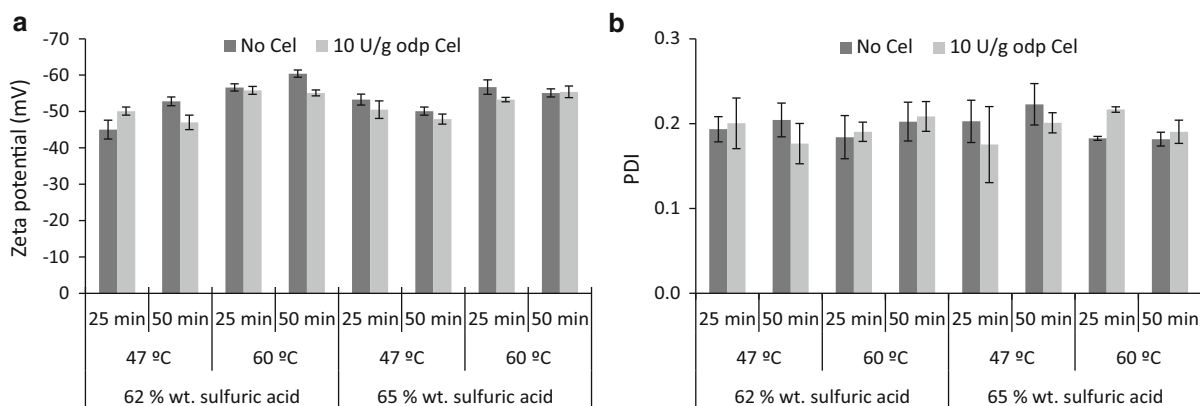


Fig. 4 Zeta potential (a) and polydispersity index (PDI) (b) of samples at studied conditions in presence and absence of cellulase

the first case, the surface charge is seen to be positively influenced by reaction time and temperature, and negatively by the interaction of cellulase and temperature. In the second case, the influences were different, with cellulase reducing the surface charge and interacting with the other two variables.

$$\begin{aligned} \text{Surface charge (meq/g)} &= 0.224 + 0.014X_2 \\ &\quad + 0.033X_3 - 0.012X_1X_3 \\ (R^2 = 0.956) &\quad (5) \end{aligned}$$

$$\begin{aligned} \text{Surface charge (meq/g)} &= 0.223 - 0.01X_1 \\ &\quad + 0.004X_3 - 0.01X_1X_2 \\ &\quad + 0.007X_1X_3 \\ (R^2 = 0.980) &\quad (6) \end{aligned}$$

The NCC surface charge increased with time and temperature for 62 wt.% sulfuric acid (Fig. 2e), probably due to higher levels of sulfate esterification at higher temperatures or longer hydrolysis times, as also observed by Chen et al. (2015). At this acid concentration, the cellulase effect was found to depend on temperature. With 65 wt.% sulfuric acid, C_NCC showed lower surface charge compared with KC_NCC, possibly due to lower sulfate esterification. Also, there seemed to be little influence of hydrolysis time and temperature on surface charge for the stronger acid dose, as observed above for NCC yield and particle size.

NCC sulfur content, stability, and polydispersity

Sulfate groups could influence several characteristics of NCC, such as its dispersibility in water suspension (Klemm et al. 2011) or thermodegradability (Roman

and Winter 2004). They may also influence the properties conferred on composites when used as filler (Moon et al. 2011). Sulfate groups on crystal surface would enable use in biomedical applications, due to the possibility of electrostatically absorbing enzymes or proteins (Lin and Dufresne 2014). NCC with no SO_4^{2-} groups on its surface, such as those obtained with enzymes (Filson et al. 2009; Anderson et al. 2014; Teixeira et al. 2015) or acids other than sulfuric (e.g., hydrobromic or hydrochloric) (Habibi et al. 2010), aggregate and flocculate in water, hindering their applicability. NCC with large sulfur content, on the other hand, would be highly susceptible to thermal degradation (Roman and Winter 2004), hindering use as filler in polymeric matrixes, which are usually manipulated at high temperatures (Hubbe et al. 2008). The sulfur content of the samples is shown in Fig. 3, where one can observe, firstly, that the higher acid concentration led to higher sulfur content, as a result of the greater extent of esterification, as previously reported in literature (Beltramino et al. 2015a; Chen et al. 2015). Secondly, the influence of cellulase on the NCC sulfation was found to depend upon other conditions. Generally, we observed that it seemed to produce an opposite effect at lower and higher acid concentrations, seeming to reduce sulfation in the former and increase it in the latter case. Lastly, concerning hydrolysis time and temperature, no remarkable influence was found with 62 wt.% acid, while with 65 wt.% acid they reduced the NCC sulfur content when increased. This observed desulfation was attributed to degradation of NCC to sugars due to excessive depolymerization (Chen et al. 2015).

Table 3 Model verification

New experimental values and those predicted by the models for optimal hydrolysis conditions (25 min, 47 °C, 62 wt.% sulfuric acid)	Optimal conditions			
	10 U/g odp cellulase		0 U/g odp cellulase	
	Experimental	Predicted ^a	Experimental	Predicted ^a
Yield (%)	82.8 ± 1.1	83.4	72.4 ± 1.2	74.2
Z average (nm)	186.4 ± 9.5	199.6	174.2 ± 19.1	199.6
Surface charge (meq/g)	0.185 ± 0.02	0.165	0.180 ± 0.018	0.189
Sulfur content (% S)	0.82 ± 0.04	1.1 ± 0.21	0.93 ± 0.03	1.21 ± 0.3
Zeta potential (mV)	−49.6 ± 1.1	−50.1 ± 1.1	−49.8 ± 0.8	−45 ± 2.6
PDI	0.17 ± 0.02	0.20 ± 0.03	0.19 ± 0.03	0.19 ± 0.02

^a Where no model was found fitting data, previous experimental value is indicated

Zeta potential, measured via electrophoretic mobility, is an indicator of the stability of colloidal suspensions (Filson et al. 2009; Alves et al. 2014). As indicated in Fig. 4a, all the studied hydrolysis conditions led to values between −45 and −60 mV, considered to indicate very high stability (Alves et al. 2014). Only slight differences were found among the samples, only revealing an increase in stability with increasing hydrolysis severity. These results indicate that NCC suspensions with good stability were obtained independently of conditions, highlighting another benefit of combined treatment with enzyme plus sulfuric acid hydrolysis.

The polydispersity index (PDI) is a measure of the heterogeneity of particle sizes within a sample, with smaller values indicating greater homogeneity. It is known that high particle size homogeneity, i.e., narrow particle size distribution, is an indicator of good quality of NCC samples (Moon et al. 2011) and is therefore a desirable feature. Also, homogeneity is a necessary feature for application of NCC as a standardized component (Moon et al. 2011). As illustrated in Fig. 4b, all samples had PDI values around 0.2, indicating homogeneous particle size distributions.

Optimal point and model verification

The objective of the present work is to find the hydrolysis conditions producing the highest NCC yield. Thus, the optimal point was defined as that providing the maximal yield. From the obtained statistical models, we found these conditions to be: cellulase presence ($X_1 = 1$), 25 min of hydrolysis ($X_2 = -1$), and 47 °C ($X_3 = -1$). At these conditions, a yield of 83.4 % was predicted by the model.

These conditions also provided a maximal yield value of 74.2 % in absence of cellulase, which is lower than the former value and therefore considerably less interesting. Comparing these conditions with those used in previous studies (Beltramino et al. 2015a), one can notice that a reduction of 20 min (i.e., 44 %) in acid hydrolysis time was achieved. Also, these optimized conditions led to a yield more than 10 % higher than that obtained in previous work, possibly by reducing unnecessary cellulose depolymerization.

The optimal yield is also significantly higher than other reported values. Recently, Fan and Li (2012) reported a ~62 % optimal yield from cotton fibers and Martínez-Sanz et al. (2015) reported ~77 % yield for NCC, also derived from pure cellulosic sources, both using a similar procedure for yield measurement. Other innovative preparation methods such as ultrasonic-assisted hydrolysis (Tanaka et al. 2014) offered ~40 % yield. At the optimal conditions, the models also predicted NCC size of around 200 nm, larger than other observed values, a fact that would reduce the toxicity (Yanamala and Farcas 2014). Also, at this point, the surface charge was among the lowest values, indirectly indicating low sulfate presence on the NCC surface, reducing the thermodegradability (Roman and Winter 2004). Finally, the zeta potential and polydispersity index values provide evidence that the optimal point also provided a sample with high stability and narrow size distribution.

To confirm the accuracy of the obtained models, new samples were prepared using the optimal hydrolysis conditions in presence and absence of cellulase. Table 3 indicates these new experimental values as well as those predicted by the models. As can be observed, the models successfully predicted the

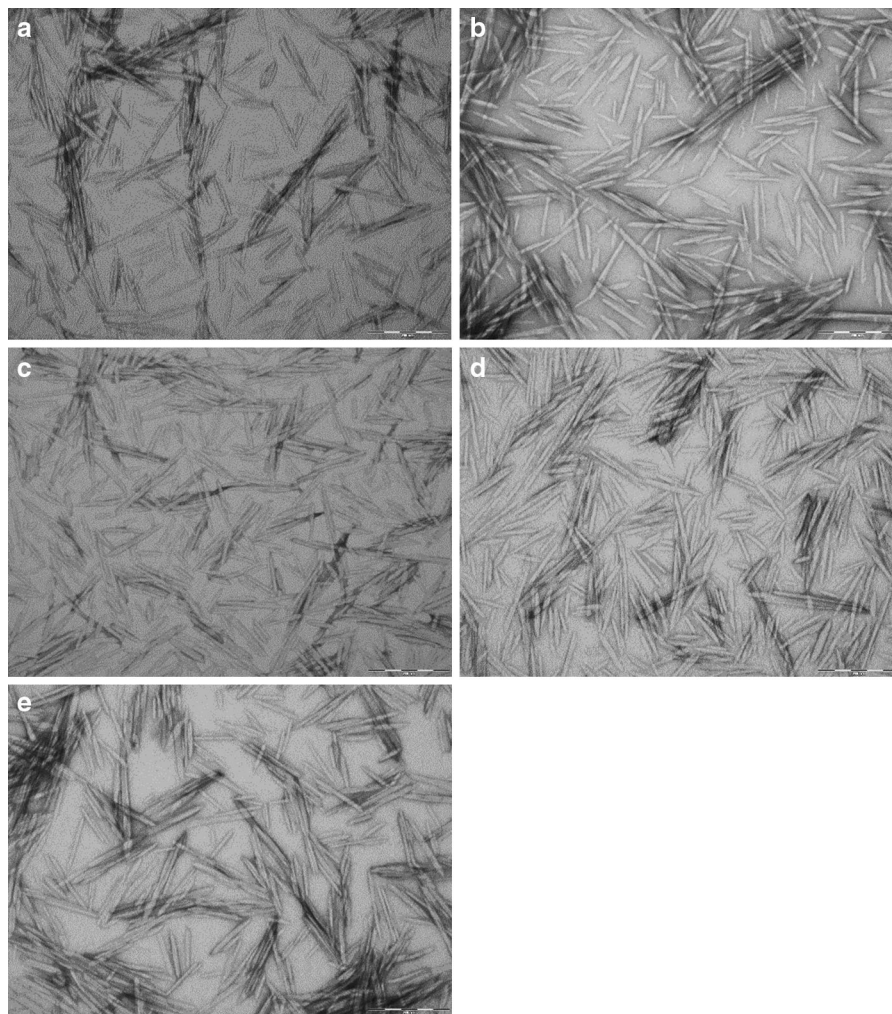


Fig. 5 TEM images of NCC corresponding to: cellulase, 25 min, 47 °C, 62 wt.% acid (optimal point, **a**); control, 25 min, 47 °C, 62 wt.% acid (**b**); cellulase, 50 min, 60 °C,

62 wt.% acid (**c**); cellulase, 25 min, 47 °C, 65 wt.% acid (**d**); cellulase, 50 min, 47 °C, 65 wt.% acid (**e**). Scale bar 100 nm

experimental data for yield, surface charge, and average size within the confidence intervals, only showing a small bias (<5 nm) in the latter case. Concerning unmodeled parameters, new values were also similar to former ones, with only small discrepancies in parameters showing higher variability among samples, such as sulfur content or zeta potential.

TEM analysis

Transmission electron microscopy (TEM) images of individual NCC particles are shown in Fig. 5. Firstly,

these images confirm the achievement of rod-shaped nanostructure (NCC) at the optimal as well as other studied conditions. Secondly, in agreement with the DLS data, the images of NCC obtained at the optimal conditions in presence and absence of cellulase pretreatment (Fig. 5a, b) seemed to show the largest particles, with no observable differences between the two samples. The images in Fig. 5c–e seem to show NCC particles with smaller size. This effect was also predicted by DLS data and can be explained by the greater severity of hydrolysis caused by longer hydrolysis time, higher temperature, or higher acid concentration, as presented above.

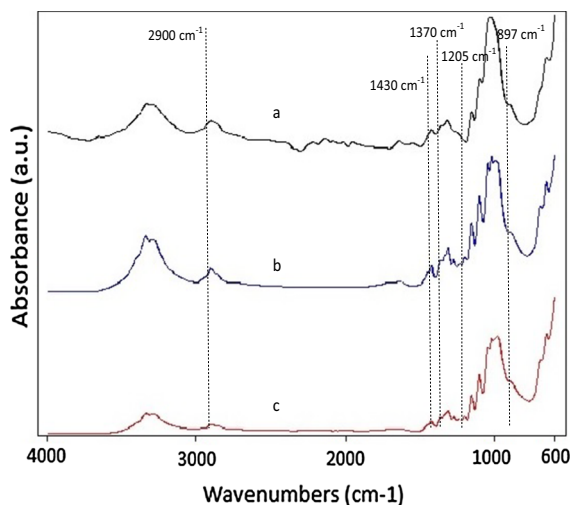


Fig. 6 FTIR spectra of (a) cellulase-pretreated fibers, (b) NCC (no cellulose, 62 wt.% acid, 25 min), and (c) NCC (cellulose, 65 wt.% acid, 50 min)

FTIR analysis

Figure 6 shows example FTIR spectra for cellulose fibers and extracted NCC. In these three cases, the spectra appear to be very similar, attending the fact that the chemical composition of the samples (pure cellulose) remained unchanged during all the studied processes. The main differences seen are related to peak intensity. Typical bands of cellulose are observed (Široký et al. 2010). The broad absorption band in the range of 3600 to 3100 cm^{-1} is mainly due to stretching of $-\text{OH}$ groups of cellulose, with typical sharpening around 3400 cm^{-1} (Široký et al. 2010; Alves et al. 2014). The peak at 2900 cm^{-1} appears due to C–H stretching of cellulose (Fahma et al. 2010). The band at 1650 to 1600 cm^{-1} originates from the bending mode of water absorbed on cellulose (i.e., moisture water) (Fahma et al. 2010). From 1800 to

600 cm^{-1} , anhydroglucopyranose vibration modes (deformation, wagging, and twisting) are seen (Alves et al. 2014). Among these, the absorption at 1044 cm^{-1} is mainly attributed to C–O stretching of C–O–C linkages, and the band at 895 cm^{-1} to C–H deformation of β -glycosidic linkages between glucose units (Alves et al. 2014). Presence of sulfate groups on NCC, not present on the original fibers, is illustrated by a small peak at 1205 cm^{-1} , which can be attributed to S=O linkage vibration, as previously described (Lu and Hsieh 2010; Neto et al. 2013). This tiny peak appears in spectra for NCC samples but seems to be absent for the original fibers (Fig. 6).

It has been reported that segments of the cellulose polymer will vibrate differently in well-ordered crystalline regions compared with amorphous phases, permitting assignment of absorption bands to crystalline or amorphous regions and allowing calculation of two different crystallinity indexes: The lateral order index (LOI), being the absorption ratio of bands at 1430 cm^{-1} (characteristic of crystalline areas) to 890 cm^{-1} (representing amorphous regions), is correlated to the overall degree of order in cellulose (O'Connor et al. 1958). The total crystallinity index (TCI), meanwhile, is calculated from the ratio of absorption peaks at 1370 and 2900 cm^{-1} and claimed to be proportional to the cellulose crystallinity index (Nelson and O'Connor 1964). Cellulose crystallinity determination is important due to its impact on the characteristics of cellulose in applications. The crystallinity index is determined by the proportion of crystalline versus amorphous regions, also being affected by the different possible spatial arrangements of the polymer (French and Santiago Cintrón 2013). Likewise, the cellulose crystallinity index has been related to the size of crystalline domains (French and Santiago Cintrón 2013), a matter of great importance in NCC preparation. Table 4 presents the TCI and LOI

Table 4 Total crystallinity index (TCI) and lateral order index (LOI) of fibers and NCC

Cellulase dose	Cellulose fibers		NCC			
	0 U/g odp	10 U/g odp	0 U/g odp		10 U/g odp	
Acid dose	—	—	62 wt.%	65 wt.%	62 wt.%	65 wt.%
TCI	0.69	0.92	1.46	0.79	2.01	1.29
LOI	1.02	0.67	0.33	0.31	0.36	0.5

Data for NCC obtained at 25 min and 60 °C

values for the fibers and NCC samples. For the fibers, it can be seen that the TCI increased after enzymatic treatment, suggesting an increase in fiber crystallinity, possibly as a consequence of preferential attack of cellulase on amorphous regions (Ahola et al. 2008). The decrease of the other studied index (LOI) in fibers, as a consequence of enzyme action, indicates a reduction in the overall order degree of cellulose, which could be related to increased accessibility of the cellulose surface (Spiridon et al. 2010). This change in the LOI value is consistent with previous observations, and could help explain the improved outcome of sulfuric acid hydrolysis of enzymatically pretreated compared with untreated fibers. Regarding NCC (Table 4), firstly, we observed higher TCI values for all samples compared with their original fibers, a consequence of removal of amorphous regions during acid hydrolysis. Secondly, we observed that the greater cellulose depolymerization produced by the higher acid dose reduced the TCI values for NCC, probably because of the well-known reduction in crystal size (French and Santiago Cintrón 2013). Lastly, cellulase pretreatment increased the TCI of NCC, possibly due to the greater presence of crystalline cellulose in NCC and/or increased size of these regions. The FTIR data suggest that a more accessible and crystalline cellulose structure of cellulose fibers was obtained as a consequence of cellulase action. These modifications might result in cleaner and more rapid access of sulfuric acid to more abundant crystalline regions, reducing sample loss in the acid hydrolysis process and providing larger NCC particles with higher crystallinity. This evidence is also in accordance with the proposed mechanism underlying the NCC yield increase produced by cellulase.

Conclusions

The results presented in this work allow determination of the optimal chemical conditions to maximize the NCC isolation yield from enzymatically pretreated fibers, obtaining values above 80 % and an increase due to the enzyme of 9 %. Also, this optimization permits substantial reduction of the hydrolysis time (by 44 %) and a yield increase of more than 10 % compared with conditions used in previous work. We found that, at the optimal conditions, the particle size remained nanoscale and the surface charge as well as

sulfur content were reduced. The results also indicate that all the sample suspensions had good stability and narrow particle size distribution. The effects of cellulase were noticeable even at high acid concentration, highlighting the potential of this pretreatment. TEM analysis confirmed the presence of NCC even under the milder hydrolysis conditions, while FTIR measurements indicated that cellulase treatment increased the crystallinity of the fibers and NCC as well as the accessibility of fibers. The conditions determined in this study will permit better usage of raw materials for NCC production, reducing unnecessary biomass consumption while maintaining product quality.

Acknowledgments Authors are grateful to Ministerio de Economía y Competitividad (Spain) for support of this work under the BIOSURFACEL (CTQ2012-34109, funding also from the Fondo Europeo de Desarrollo Regional, FEDER) and BIOPAPμFLUID (CTQ2013-48995-C2-1-R) projects and an FPI grant (BES-2011-046674). Special thanks are also due to the consolidated research group AGAUR 2014 SGR 534 with Universitat de Barcelona (UB). We are also grateful to Celsur and Fungal Bioproducts for supplying cotton linters and enzyme, respectively.

References

- Abitbol T, Kloser E, Gray DG (2013) Estimation of the surface sulfur content of cellulose nanocrystals prepared by sulfuric acid hydrolysis. *Cellulose* 20:785–794
- Ahola S, Turon X, Osterberg M et al (2008) Enzymatic hydrolysis of native cellulose nanofibrils and other cellulose model films: effect of surface structure. *Langmuir* 24:11592–11599. doi:[10.1021/la801550j](https://doi.org/10.1021/la801550j)
- Alves L, Medronho B, Antunes FE et al (2014) Unusual extraction and characterization of nanocrystalline cellulose from cellulose derivatives. *J Mol Liq*. doi:[10.1016/j.molliq.2014.12.010](https://doi.org/10.1016/j.molliq.2014.12.010)
- Anderson SR, Esposito D, Gillette W et al (2014) Enzymatic preparation of nanocrystalline and microcrystalline cellulose. *Tappi J* 13:35–42
- Beltramino F, Roncero MB, Vidal T et al (2015a) Increasing yield of nanocrystalline cellulose preparation process by a cellulase pretreatment. *Bioresour Technol* 192:574–581. doi:[10.1016/j.biortech.2015.06.007](https://doi.org/10.1016/j.biortech.2015.06.007)
- Beltramino F, Valls C, Vidal T, Roncero MB (2015b) Exploring the effects of treatments with carbohydrases to obtain a high-cellulose content pulp from a non-wood alkaline pulp. *Carbohydr Polym* 133:302–312. doi:[10.1016/j.carbpol.2015.07.016](https://doi.org/10.1016/j.carbpol.2015.07.016)
- Brinchi L, Cotana F, Fortunati E, Kenny JM (2013) Production of nanocrystalline cellulose from lignocellulosic biomass: technology and applications. *Carbohydr Polym* 94:154–169. doi:[10.1016/j.carbpol.2013.01.033](https://doi.org/10.1016/j.carbpol.2013.01.033)

- Chen L, Wang Q, Hirth K et al (2015) Tailoring the yield and characteristics of wood cellulose nanocrystals (CNC) using concentrated acid hydrolysis. *Cellulose*. doi:[10.1007/s10570-015-0615-1](https://doi.org/10.1007/s10570-015-0615-1)
- Dong XM, Revol J-F, Gray DG (1998) Effect of microcrystallite preparation conditions on the formation of colloid crystals of cellulose. *Cellulose* 5:19–32
- Fahma F, Iwamoto S, Hori N et al (2010) Isolation, preparation, and characterization of nanofibers from oil palm empty-fruit-bunch (OPEFB). *Cellulose* 17:977–985. doi:[10.1007/s10570-010-9436-4](https://doi.org/10.1007/s10570-010-9436-4)
- Fan JS, Li YH (2012) Maximizing the yield of nanocrystalline cellulose from cotton pulp fiber. *Carbohydr Polym* 88:1184–1188. doi:[10.1016/j.carbpol.2012.01.081](https://doi.org/10.1016/j.carbpol.2012.01.081)
- Filson PB, Dawson-Andoh BE, Schwegler-Berry D (2009) Enzymatic-mediated production of cellulose nanocrystals from recycled pulp. *Green Chem* 11:1808. doi:[10.1039/b915746h](https://doi.org/10.1039/b915746h)
- Fraschini C, Chauve G, Le Berre J-F et al (2014) Critical discussion of light scattering and microscopy techniques for CNC particle sizing. *Nord Pulp Pap Res J* 29:31–40
- French AD, Santiago Cintrón M (2013) Cellulose polymorphy, crystallite size, and the Segal Crystallinity Index. *Cellulose* 20:583–588. doi:[10.1007/s10570-012-9833-y](https://doi.org/10.1007/s10570-012-9833-y)
- Habibi Y, Lucia LA, Rojas OJ (2010) Cellulose nanocrystals: chemistry, self-assembly, and applications. *Chem Rev* 110:3479–3500. doi:[10.1021/cr900339w](https://doi.org/10.1021/cr900339w)
- Hubbe MA, Rojas OJ, Lucia LA, Sain M (2008) Cellulosic nanocomposites: a review. *BioResources* 3:929–980
- Klemm D, Kramer F, Moritz S et al (2011) Nanocelluloses: a new family of nature-based materials. *Angew Chem Int Ed* 50:5438–5466. doi:[10.1002/anie.2011001273](https://doi.org/10.1002/anie.2011001273)
- Lin N, Dufresne A (2014) Nanocellulose in biomedicine: current status and future prospect. *Eur Polym J* 59:302–325. doi:[10.1016/j.eurpolymj.2014.07.025](https://doi.org/10.1016/j.eurpolymj.2014.07.025)
- Lu P, Hsieh Y-L (2010) Preparation and properties of cellulose nanocrystals: rods, spheres, and network. *Carbohydr Polym* 82:329–336. doi:[10.1016/j.carbpol.2010.04.073](https://doi.org/10.1016/j.carbpol.2010.04.073)
- Martínez-Sanz M, Vicente AA, Gontard N et al (2015) On the extraction of cellulose nanowhiskers from food by-products and their comparative reinforcing effect on a polyhydroxybutyrate-co-valerate polymer. *Cellulose* 22:535–551. doi:[10.1007/s10570-014-0509-7](https://doi.org/10.1007/s10570-014-0509-7)
- Moon RJ, Martini A, Nairn J et al (2011) Cellulose nanomaterials review: structure, properties and nanocomposites. *Chem Soc Rev* 40:3941–3994. doi:[10.1039/c0cs00108b](https://doi.org/10.1039/c0cs00108b)
- Nelson ML, O'Connor RT (1964) Relation of certain infrared bands to cellulose crystallinity and crystal lattice type. Part II. A new infrared ratio for estimation of crystallinity in celluloses I and II. *J Appl Polym Sci* 8:1325–1341. doi:[10.1002/app.1964.070080323](https://doi.org/10.1002/app.1964.070080323)
- Neto WPF, Silvério HA, Dantas NO, Pasquini D (2013) Extraction and characterization of cellulose nanocrystals from agro-industrial residue - Soy hulls. *Ind Crops Prod* 42:480–488. doi:[10.1016/j.indcrop.2012.06.041](https://doi.org/10.1016/j.indcrop.2012.06.041)
- O'Connor RT, DuPré EF, Mitcham D (1958) Applications of infrared absorption spectroscopy to investigations of cotton and modified cottons part I: physical and crystalline modifications and oxidation. *Text Res J* 28:382–392. doi:[10.1177/004051755802800503](https://doi.org/10.1177/004051755802800503)
- Quintana E, Valls C, Vidal T, Roncero MB (2015a) Comparative evaluation of the action of two different endoglucanases. Part II: on a biobleached acid sulphite pulp. *Cellulose* 22:2081–2093. doi:[10.1007/s10570-015-0631-1](https://doi.org/10.1007/s10570-015-0631-1)
- Quintana E, Valls C, Vidal T, Roncero MB (2015b) Comparative evaluation of the action of two different endoglucanases. Part I: on a fully bleached, commercial acid sulfite dissolving pulp. *Cellulose*. doi:[10.1007/s10570-015-0623-1](https://doi.org/10.1007/s10570-015-0623-1)
- Roman M, Winter WT (2004) Effect of sulfate groups from sulfuric acid hydrolysis on the thermal degradation behavior of bacterial cellulose. *Biomacromolecules* 5:1671–1677. doi:[10.1021/bm034519+](https://doi.org/10.1021/bm034519+)
- Široký J, Blackburn RS, Bechtold T et al (2010) Attenuated total reflectance Fourier-transform infrared spectroscopy analysis of crystallinity changes in lyocell following continuous treatment with sodium hydroxide. *Cellulose* 17:103–115. doi:[10.1007/s10570-009-9378-x](https://doi.org/10.1007/s10570-009-9378-x)
- Spiridon I, Teaca C-A, Bodîrlau R (2010) Structural changes evidenced by FTIR spectroscopy in cellulosic materials after pre-treatment with ionic liquid and enzymatic hydrolysis. *BioResources* 6:400–413
- Tanaka R, Saito T, Ishii D, Isogai A (2014) Determination of nanocellulose fibril length by shear viscosity measurement. *Cellulose* 21:1581–1589. doi:[10.1007/s10570-014-0196-4](https://doi.org/10.1007/s10570-014-0196-4)
- Teixeira RSS, da Silva AS, Jang J-H et al (2015) Combining biomass wet disk milling and endoglucanase/β-glucosidase hydrolysis for the production of cellulose nanocrystals. *Carbohydr Polym* 128:75–81. doi:[10.1016/j.carbpol.2015.03.087](https://doi.org/10.1016/j.carbpol.2015.03.087)
- Thielemans W, Warbey CR, Walsh DA (2009) Permselective nanostructured membranes based on cellulose nanowhiskers. *Green Chem* 11:531–537. doi:[10.1039/b818056c](https://doi.org/10.1039/b818056c)
- Valls C, Roncero MB (2009) Using both xylanase and laccase enzymes for pulp bleaching. *Bioresour Technol* 100:2032–2039. doi:[10.1016/j.biortech.2008.10.009](https://doi.org/10.1016/j.biortech.2008.10.009)
- Valls C, Colom JF, Baffert C et al (2010) Comparing the efficiency of the laccase–NHA and laccase–HBT systems in eucalyptus pulp bleaching. *Biochem Eng J* 49:401–407. doi:[10.1016/j.bej.2010.02.002](https://doi.org/10.1016/j.bej.2010.02.002)
- Wang QQ, Zhu JY, Reiner RS et al (2012) Approaching zero cellulose loss in cellulose nanocrystal (CNC) production: recovery and characterization of cellulosic solid residues (CSR) and CNC. *Cellulose* 19:2033–2047. doi:[10.1007/s10570-012-9765-6](https://doi.org/10.1007/s10570-012-9765-6)
- Yanamala N, Farcas M (2014) In vivo evaluation of the pulmonary toxicity of cellulose nanocrystals: a renewable and sustainable nanomaterial of the future. *ACS Sustain Chem Eng* 2:1691–1698